ISSN 0967-0912, Steel in Translation, 2022, Vol. 52, No. 3, pp. 290–295. © Allerton Press, Inc., 2022.
Russian Text © The Author(s), 2022, published in Izvestiya Vysshikh Uchebnykh Zavedenii, Chernaya Metallurgiya, 2022, No. 3, pp. 209–215.

Transformation of Structural-Phase States in the Rail Head after Extremely Long-Term Operation

R. V. Kuznetsov[a, *], **V. E. Kormyshev**[a, **] (ORCID: 0000-0002-5147-5343), **V. E. Gromov**[a, ***] (ORCID: 0000-0002-5147-5343), **Yu. F. Ivanov**[b, ****] (ORCID: 0000-0001-8022-7958), and **Yu. A. Shlyarova**[a, *****] (ORCID: 0000-0001-5677-1427)

[a] *Siberian State Industrial University (SibSIU), Novokuznetsk, Kemerovo Region, Kuzbass, 654007 Russia*
[b] *Institute of High Current Electronics of the Siberian Branch of the Russian Academy of Sciences (IHCE SB RAS), Tomsk, 634055 Russia*

**e-mail: mail@kuzmash.com*
***e-mail: 89236230000@mail.ru*
****e-mail: gromov@physics.sibsiu.ru*
*****e-mail: yufi55@mail.ru*
******e-mail: rubannikova96@mail.ru*

Received July 12, 2021; revised August 30, 2021; accepted September 27, 2021

Abstract—At the macro-, micro- and nanoscale levels, the optical, scanning and transmission electron diffraction microscopy methods revealed quantitative transformations of the structure at a depth of 0, 2, 5, 10 mm along the central axis and the symmetry axis of the head fillet of long-length differentially hardened rails after extremely long-term operation (passed tonnage 1770 million gross tons). At the macroscale level, numerous shallow parallel contact fatigue cracks are observed on the surface of the working fillet, and small spalls are observed on the surface of the non-working fillet. The side wear of the rail was 2.5 mm, and the vertical wear was 2 mm. The metal microstructure of the rail head complies with the requirements of the standard and technical specifications of Russian Railways. At the microscale level, the transformation of cementite plates was established by cutting them with moving dislocations and dissolving with the escape of carbon to the dislocation lines, low- and high-angle boundaries. There is a decrease in the dispersion of the microstructure with distance from the tread surface. At the nanoscale level, the subgrain structure formed in the surface layers (subgrain size 110–200 μm) contains nanosized cementite particles (25–60 nm) localized at the joints and along the subgrain boundaries. It is suggested that this type of structure is formed as a result of dynamic recrystallization during megaplastic deformation, which occurs during extremely long-term operation of rails. The content of the subgrain structure in the fillet layer is five times higher than the content in the surface layer of the tread surface. It has been established that during operation, the transformation of lamellar perlite along the central axis of the head proceeds more slowly than along the symmetry axis of the fillet.

Keywords: scale levels, structure, evolution, rails, tread surface, fillet

DOI: 10.3103/S0967091222030081

INTRODUCTION

The service life of rails is determined by many factors: metal purity, structure, phase composition, operating conditions, heat treatment technology, etc. In rails at modern speeds of movement of trains and high contact pressures, even with a relatively small passed tonnage in the surface layers, a strong change in the structure is observed, and also an anomalously high microhardness and the phenomenon of cementite decomposition are noted. During long-term operation, numerous defects accumulate in the rails, segregation, relaxation, homogenization and recrystallization processes are induced. Phase transitions may be accompanied by a deterioration in physical and mechanical properties and may also cause failure of the rails [1].

An analysis of studies on the problem of the formation of structural-phase states in rails during long-term operation allows us to state that this problem is one of the key ones for the physics of condensed matter [2].

In [1, 2], a data bank was formed on the regularities of the formation of structural-phase states and dislocation substructure, the distribution of carbon atoms in the head of long-length differentially hardened rails along the central axis and along the fillet after long-

Table 1. Chemical composition of rail metal of DT350 category

Material	Content, % (by mass)											
	C	Mn	Si	P	S	Cr	Ni	Cu	Al	Ti	Mo	V
Sample	0.73	0.75	0.58	0.012	0.007	0.42	0.07	0.13	0.002	0.003	0.006	0.04
TU requirements	0.71–0.82	0.75–1.25	0.25–0.60	No more 0.020	0.020	0.20–0.80	With a total share of not more than 0.27 ≤0.20	≤0.20	No more than 0.004	No more than 0.010	–	0.03–0.15

term operation (passed tonnage 691 and 1411 million gross tons). To date, a batch of DT350 rails produced in 2013 at EVRAZ ZSMK JSC has reached an unprecedented in Russian practice of 1770 million tons of gross tonnage passed at the at Experimental Ring of JSC Russian Railway Research Institute (VNIIZhT).

In foreign literature, researchers limit themselves to studying the structure and properties of rails after a small amount of tonnage passed [3, 4]. They analyze the formation of a white layer [5–8], the mechanisms of nanostructure formation in the surface layer of a rail [9], a contact fatigue crack, and the distribution of tread surface irregularities [10, 11].

The purpose of this work is to study the changes in the structure and phase composition in the head of 100-meter differentially hardened rails after extreme operation on the railway (tonnage passed 1770 million gross tons) at various scale levels.

MATERIAL AND RESEARCH METHODS

As a research material, samples were taken from the R65 rail of the DT350 category made of steel grade E76HF, taken from the track at the Experimental Site in Shcherbinka. The rail was withdrawn from the track after passing 1770 million tons of gross weight due to a defect classified in accordance with the instruction [12] under code 11.2 (cracks and spalling of metal on the side working fillet or on the middle part of the head, which arose from the inside from local accumulations of non-metallic inclusions elongated along the rolling direction in the form of tracks-lines or arising from the outer surface of the rail due to insufficient contact fatigue strength of the rail metal). The chemical composition of the metal of the investigated rail, determined by spectral and chemical methods, as well as the requirements of TU 0921-276-01124323–2012 for steel grade E76HF, are given in Table 1.

Metal macrostructure was revealed by deep etching in 50% aqueous hydrochloric acid solution at a distance of about 40 mm from the spalling zone. Rail metal microstructure was studied by optical and scanning electron microscopy (SEM) on thin sections cut outside the defective zone in accordance with the requirements of TU 0921-276-01124323–2012. The defective metal substructure was studied by transmission electron diffraction microscopy (TEM) [13–17]. As in [1, 2], the objects of study for the transmission electron microscope were prepared by thinning the plates cut from the bulk workpiece at a distance of 2 and 10 mm from the rail surface (tread surface and working fillet), as well as from a plate adjacent to the surface of rail.

RESEARCH RESULTS AND DISCUSSIONS

The metal macrostructure of the test sample in terms of center segregation, point inhomogeneity, segregation stripes and cracks was studied on a macrotemplate. As a result of the performed studies, no internal defects nor discontinuities were revealed. The side wear of the rail was 2.5 mm, and the vertical wear was 2 mm. On the surface of the working fillet of the head, numerous parallel cracks of contact fatigue were revealed. On the surface of the non-working fillet, small spalling was revealed, passing in a strip up to 5 mm wide along thin winding cracks. In the place of numerous parallel surface cracks of contact fatigue, as well as in the place of small spallings on the macrotemplate from the surface of the head, discontinuities up to approximately 0.5 mm deep are observed.

Studies of the microstructure of rail metal revealed grains of lamellar pearlite and, in a small amount, areas of ferrite; bainite is absent in the microstructure (Fig. 1). Thus, the microstructure of the base metal in the examined rail head meets the requirements of the standard.

An analysis of the metal microstructure of the studied rail at a depth of 2, 5, and 10 mm from the

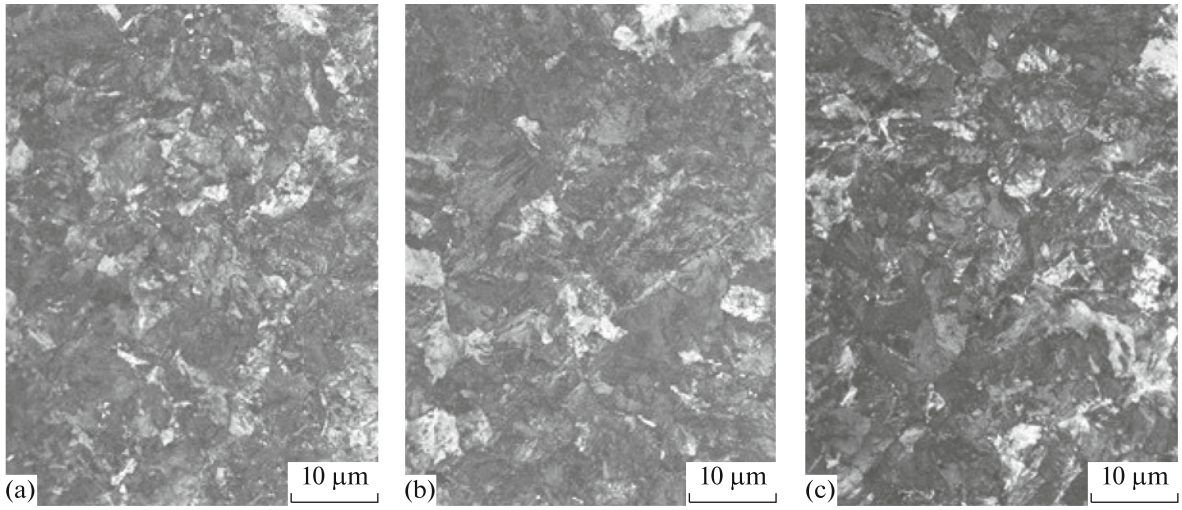

Fig. 1. Microstructure of the metal in the head of the investigated rail at a depth of 2 (a), 5 (b) and 10 mm (c) from the tread surface along the vertical axis.

tread surface along the vertical axis and along the billetradius of the fillet surface showed that the dispersity of the microstructure decreases with distance from the surface.

More detailed studies of the metal microstructure of the rail head by scanning electron microscopy showed that the microstructure of the metal is formed by grains of highly dispersed perlite with insignificant areas of structurally free ferrite (Fig. 2). The main share of perlite is regular colonies with right alternation of cementite and ferrite plates. In the fillet zone and the middle part of the rail head, a significant amount of pearlite colonies with curved (wavy) and collapsed cementite plates, as well as areas of degenerated pearlite, are observed in the microstructure.

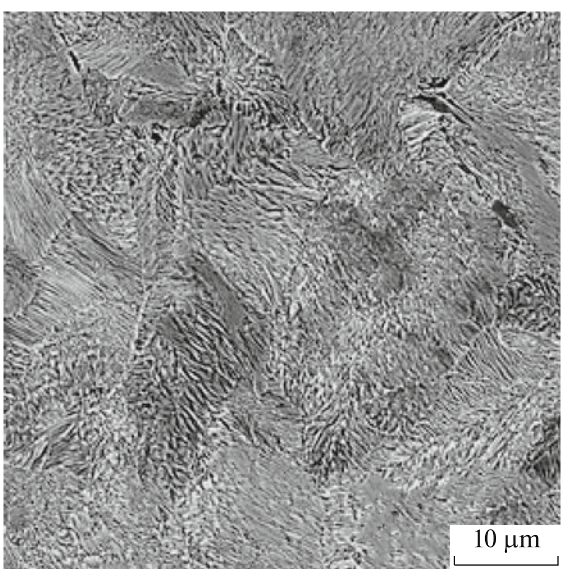

Fig. 2. Metal microstructure in the head of the investigated rail at a depth of 2 mm. Scanning electron microscopy of an etched section.

TEM studies of the metal structure of the head made it possible to detail the structural-phase state of pearlite in the studied sample. It was found that, regardless of the direction of the study (along the billetradius of the fillet or along the central axis of the head), there are several structural states of pearlite in the steel, which are classified according to the morphological feature as follows:

— firstly, this is a pearlite structure of lamellar morphology with alternating of parallel plates of cementite and ferrite (Fig. 3a);

— secondly, perlite is destroyed, in which there are no extended plates of cementite. They are fragmented and shifted relative to the original axial line (Fig. 3b). Such a structure is formed as a result of shearing and shifting of cementite plates by moving dislocations [18, 19];

— third, a ferrite-carbide mixture (degenerate pearlite) in which cementite particles of different shapes and sizes are arranged chaotically in the ferrite grains (Fig. 3c).

— fourth, ferrite grains with a band substructure organized by low-angle boundaries (Fig. 3d). Cementite in such grains is present in the form of rounded particles located along low-angle boundaries.

Ferrite grains with a fragmented (subgrain) structure are observed on the tread surfaces and the working fillet (Fig. 4). Rounded cementite particles 25–60 nm in size are located at the joints and along the boundaries of subgrains 110–200 nm in size. It can be assumed that this type of structure was formed as a result of dynamic recrystallization of steel under severe

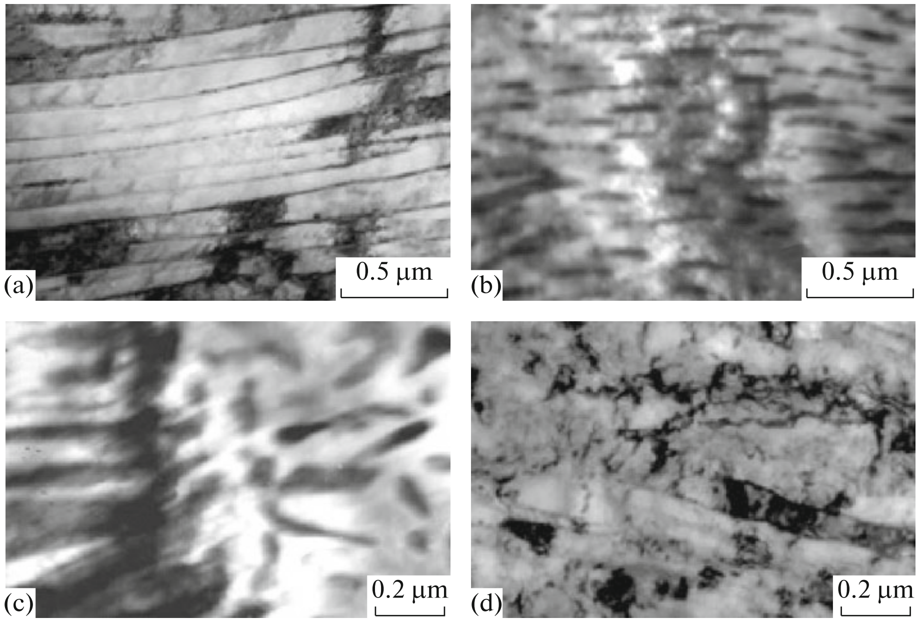

Fig. 3. Electron microscopic image of the metal structure of the rail head.

plastic deformation and cyclic loading of the rail metal during long-term operation [20].

The relative content of the identified morphological varieties of the metal structure using stereological methods is shown in Fig. 5.

It can be seen that the transformation of the pearlite structure of lamellar morphology relative to the central axis during operation proceeds much more slowly compared to the change in the structure relative to the billetradius of the working fillet. The subgrain structure is formed mainly in the surface layer of the rail. The relative content of the subgrain structure in the surface layer of the working fillet is five times higher than in the surface layer of the tread surface. The foregoing indicates a significantly higher level of transformation of the metal structure along the radius of the working fillet compared to the metal along the central axis.

CONCLUSIONS

Methods of optical, scanning and transmission electron microscopy have been used to study structure and phase composition in the head of long-gauge differentially hardened rails after the passed tonnage of 1770 million tons at different structural and scale levels. The formation of rail wear (side wear in the layer with thickness of 2.5 mm, and vertical wear—2 mm) has been revealed at the macro level. Numerous parallel cracks of contact fatigue were revealed on the surface of the working fillet of the head. On the surface of the non-working fillet, the small spallings was revealed, passing by a strip up to 5 mm in width along thin winding cracks. In the place of numerous parallel surface cracks of contact fatigue, as well as in the place of shallow spallings on the macro-template from the surface of the head, discontinuities up to 0.5 mm in depth are observed.

At the micro level, a significant transformation of the structural-phase state of lamellar perlite grains was revealed, accompanied by the destruction of cementite plates by their cutting by moving dislocations and dissolution with the departure of carbon from the cementite lattice to dislocation lines, low-angle and high-angle boundaries. At the nanoscale level, the formation of a subgrain structure containing nanosized cementite particles located at the joints and along the boundaries of subgrains was revealed. The sizes of sub-

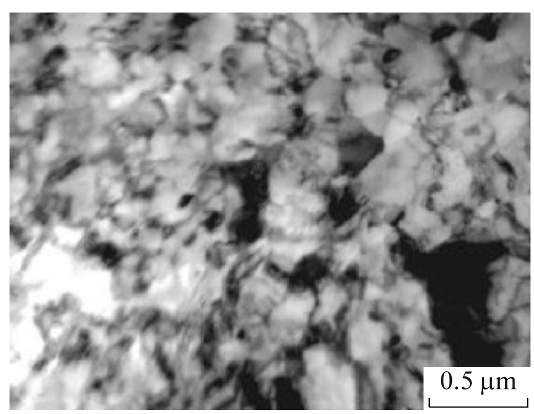

Fig. 4. Fragmented (subgrain) structure formed in the surface layer of the rail head metal.

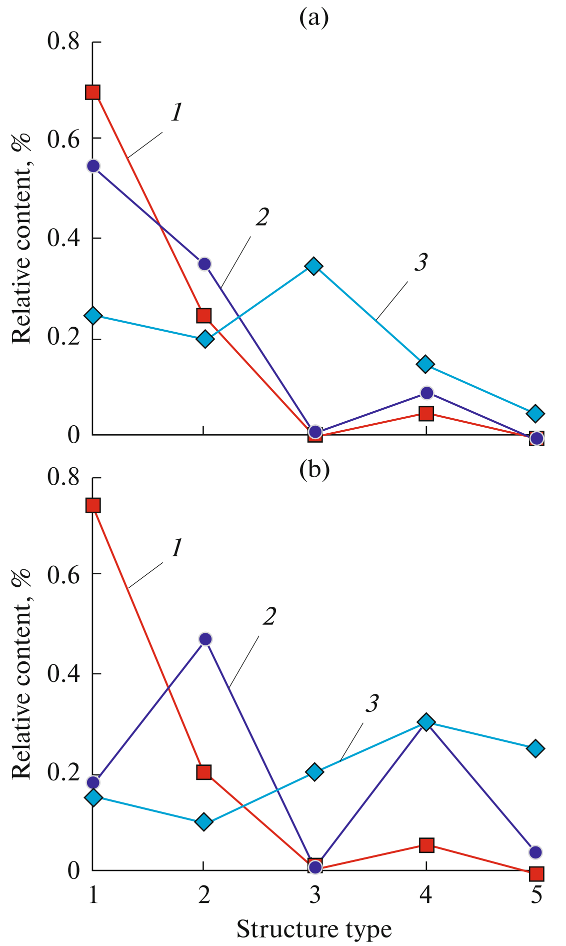

Fig. 5. Relative content of different types of metal structure of the rail head, identified along the central axis (relative to the tread surface) (a) and along the billetradius of the working fillet (b). Curves: (*1*) relative content of structure types in the layer located at a depth of 10 mm; (*2*) in a layer located at a depth of 2 mm; (*3*) in the surface layer. Structure types: (1) lamellar pearlite; (2) destroyed pearlite; (3) degenerate pearlite (ferrite-carbide mixture); (4) ferrite grains, in the volume of which a band substructure is observed; (5) ferrite grains with a fragmented (subgrain) structure.

grains vary from 110 to 200 nm, and the sizes of cementite particles vary from 25 to 60 nm. It is suggested that this type of structure is formed as a result of dynamic recrystallization of steel under cyclic loading during long-term operation of rails. It has been established that the transformation of perlite structure of lamellar morphology relative to the central axis of the head proceeds more slowly compared to the change in the structure relative to the billetradius of the working fillet. The relative content of the subgrain structure formed in the surface layer of the working fillet is five times higher than in the surface layer of the tread surface.

ACKNOWLEDGMENTS

We are grateful to E.V. Polevoi for providing of samples and to A.E. Korochkin for the participation in discussions of the results.

FUNDING

This work was supported by the Russian Foundation for Basic Research, grant no. 19-32-60001.

CONFLICT OF INTERESTS

The authors declare that they have no conflicts of interest.

REFERENCES

1. Yuriev, A.A., Gromov, V.E., Ivanov, Yu.F., Rubannikova, Yu.A., Starostenkov, M.D., and Tabakov, P.Y., *Structure and Properties of Lengthy Rails after Extreme Long-Term Operation*, Millersville, Pa.: Materials Research Society, 2021. https://doi.org/10.21741/9781644901472
2. Gromov, V.E., Ivanov, Yu.F., Kormyshev, V.E., Yuriev, A.A., Semin, A.P., and Rubannikova, Yu.A., Change in structural-phase states and properties of lengthy rails during extremely long-term operation, *Usp. Fiz. Met.*, 2020, vol. 21, no. 4, pp. 527–553. https://doi.org/10.15407/ufm.21.04.527
3. Ivanisenko, Yu. and Fecht, H.J., Microstructure modification in the surface layers of railway rails and wheels: Effect of high strain rate deformation, *Steel Tech*, 2008, vol. 3, no. 1, pp. 19–23.
4. Ivanisenko, Yu., Maclaren, I., Sauvage, X., Valiev, R.Z., and Fecht, H.-J., Shear-induced $\alpha \to \gamma$ transformation in nanoscale Fe–C composite, *Acta Mater.*, 2006, vol. 54, no. 6, pp. 1659–1669. https://doi.org/10.1016/j.actamat.2005.11.034
5. Wu, J., Petrov, R.H., Kolling, S., Koenraad, P., Malet, L., Godet, S., and Sietsma, J., Micro and nanoscale characterization of complex multilayer-structured white etching layer in rails, *Metals*, 2018, vol. 8, no. 10, pp. 749–761. https://doi.org/10.3390/met8100749
6. Zhang, H.W., Ohsaki, S., Mitao, S., Ohnuma, M., and Hono, K., Microstructural investigation of white etching layer on pearlite steel rail, *Mater. Sci. Eng., A*, 2006, vol. 421, nos. 1–2, pp. 191–199. https://doi.org/10.1016/j.msea.2006.01.033
7. Takahashi, J., Kawakami, K., and Ueda, M., Atom probe tomography analysis of the white etching layer in a rail track surface, *Acta Mater.*, 2010, vol. 58, no. 10, pp. 3602–3612. https://doi.org/10.1016/j.actamat.2010.02.030
8. Newcomb, S.B. and Stobbs, W.M., A transmission electron microscopy study of the white-etching layer on a rail head, *Mater. Sci. Eng.*, 1984, vol. 66, no. 2, pp. 195–204. https://doi.org/10.1016/0025-5416(84)90180-0
9. Lojkowski, W., Djahanbakhsh, M., Burkle, G., Gierlotka, S., Zielleski, W., and Fecht, H.-J., Nanostructure formation on the surface of railway tracks, *Mater.*

Sci. Eng., A, 2001, vol. 303, nos. 1–2, pp. 197–208. https://doi.org/10.1016/S0921-5093(00)01947-X

10. Wild, E., Wang, L., Hasse, B., Wroblewski, T., Goerigk, G., and Pyzalla, A., Microstructure alterations at the surface of a heavily corrugated rail with strong ripple formation, *Wear*, 2003, vol. 254, no. 9, pp. 876–883.
https://doi.org/10.1016/S0043-1648(03)00239-4
11. Ishida, M., Rolling contact fatigue (RCF) defects of rails in Japanese railways and its mitigation strategies, *Electron. J. Struct. Eng.*, 2013, vol. 13, no. 1, pp. 67–74. https://ejsei.com/EJSE/article/view/162.
12. Rail defects. Classification, catalog and parameters of defective and acute-defective rails. Instruction, Moscow: Order of the Russian Railways no. 2499 of October 23, 2014.
13. Kumar, C.S.S.R., *Transmission Electron Microscopy: Characterization of Nanomaterials*, New York: Springer, 2014.
https://doi.org/10.1007/978-3-642-38934-4
14. *Transmission Electron Microscopy: Diffraction, Imaging, and Spectrometry*, Carter, C.B. and Williams, D.B., Eds., Berlin: Springer, 2016.
https://doi.org/10.1007/978-3-319-26651-0
15. Egerton, F.R., *Physical Principles of Electron Microscopy: An Introduction to TEM, SEM, and AEM*, Basel: Springer, 2016.
https://doi.org/10.1007/978-3-319-39877-8
16. Tomas, G. and Goringe, M.J., *Transmission Electron Microscopy of Materials*, New York: John Wiley & Sons, 1979.
17. Hirsch, P.B., Howie, A., Nicholson, R., Pashley, D.W., and Whelan, M.J., *The Electron Microscopy of Thin Crystals*, Butterworths, 1965.
18. Gavrilyuk, V.G., Gertsriken, D.S., Polushkin, Yu.A., and Fal'chenko, V.M., Mechanism of cementite decomposition during plastic deformation of steel, *Phys. Met. Metallogr.*, 1981, vol. 51, no. 1, pp. 125–129.
19. Gridnev, V.N. and Gavrilyuk, V.G., Cementite decomposition in steel under plastic deformation (a review), *Phys. Met.*, 1982, vol. 4, no. 3, pp. 531–551.
20. Glezer, A.M., On the nature of ultrahigh plastic (megaplastic) strain, *Bull. Russ. Acad. Sci. Phys.*, 2007, vol. 71, no. 12, pp. 1722–1730.
https://doi.org/10.3103/S106287380712012X

Translated by V. Selikhanovich